Available online at www.sciencedirect.com
SCIENCE DIRECT®
Biochemical Pharmacology 68 (2004) 875–883
Biochemical Pharmacology
www.elsevier.com/locate/biochempharm

Calcium ionophoretic and apoptotic effects of ferutinin in the human Jurkat T-cell line

Antonio Macho[a], Magdalena Blanco-Molina[a], Paola Spagliardi[b], Giovanni Appendino[b,1], Paul Bremner[c], Michael Heinrich[c], Bernd L. Fiebich[d], Eduardo Muñoz[a,*]

[a]*Departamento de Biología Celular, Fisiología e Inmunología, Universidad de Córdoba, Facultad de Medicina, Avda. de Menendez Pidal s/n, E-14004 Córdoba, Spain*
[b]*DiSCAFF, Università del Piemonte Orientale, Viale Ferrucci 33, I-28100 Novara, Italy*
[c]*Centre for Pharmacognosy and Phytotherapy, The School of Pharmacy, University of London, 29-39 Brunswick Square, London WC1N 1AX, UK*
[d]*Neurochemistry Research Group, Department of Psychiatry, University of Freiburg Medical School, Hauptstrasse 5, D-79104 Germany*

Received 16 March 2004; accepted 13 May 2004

Abstract

We have investigated the ionophoretic and apoptotic properties of the daucane sesquiterpene ferutinin and three related compounds, ferutidin, 2-α-hydroxyferutidin and teferin, all isolated from various species of plants from the genus *Ferula*. Ferutinin induced a biphasic elevation of intracellular Ca^{2+} in the leukemia T-cell line, Jurkat. First, a rapid calcium peak was observed and inhibited by BAPTA-AM. This initial calcium mobilization was followed by a sustained elevation, mediated by the entry of extracellular calcium through L-type calcium channels and sensitive to inhibition by EGTA. Moreover, ferutinin-induced apoptosis in Jurkat cells, and this event was preceded, in a cyclosporine-A sensitive manner, by a loss of mitochondrial transmembrane potential ($\Delta\Psi_m$) and by an increase in intracellular reactive oxygen species. Ferutinin-induced DNA fragmentation was mediated by a caspase-3-dependent pathway, and was initiated independently of any specific phase of the cell cycle. The evaluation of ferutinin analogs in calcium mobilization and apoptosis assays showed strict structure–activity relationships, with *p*-hydroxylation of the benzoyl moiety being requested for activity.

Keywords: Ferula; Ferutinin; Ferutidin; Cytotoxicity; Apoptosis; Calcium mobilization

1. Introduction

The use of plants from the *Ferula* genus (Family *Umbelliferae*) is documented in the traditional medicine of the Mediterranean region since the Greek and Roman times. These plants are also well known for their toxicity, and modern studies have focused on the hemorrhagic activity of several prenylated 4-hydroxycoumarins from a toxic chemotype of giant fennel (*Ferula communis* L.) [1,2]. Several sesquiterpene derivatives have been isolated from the *Ferula* genus, most of which display biological activities. Ferutinin is a potent phytoestrogen which has agonist activities over the α and β subunits of human estrogen receptor [3,4]. In vivo experiments in female rats have shown that administration of ferutinin can modulate the content in luteinising hormone, whereas in male rats this compound can increase the levels of gonadotropin in the bloodstream [5]. In addition, ferutinin and its methyl derivative ferutidin have been reported to show ionophoretic properties, apparently related to their ability to increase conductance directly in phospholipid membranes and through the formation of a stoichiometric complex with calcium [6]. More recently, Abramov and Duchen have shown, using an elegant digital imaging technique, that ferutinin also induces a calcium-dependent mitochondrial depolarization [7].

Abbreviations: ac-DEVD-amc, *N*-acetyl-aspartyl-glutamyl-valyl-aspartyl-aminomethyl-coumarin; AM, acetoxy methyl ester; BAPTA-AM, 1,2-bis-(2-aminophenoxy-ethane)-*N*,*N*,*N*′,*N*′-tetraacetate tetrakis-acetoxy methyl ester; CsA, Cyclosporin-A; $\Delta\Psi_m$, mitochondrial transmembrane potential; EGTA, ethylene glycol-bis(beta-aminoethyl-ether)-*N*,*N*,*N*′,*N*′-tetraacetate; Eth, ethidium; FITC-dUTP, fluorescein isothiocyanate-12-deoxy-2-uridine triphosphate; HE, dihydroethidium; PBS, phosphate buffered saline; PI, propidium iodide; PTP, permeability transition pore; ROS, reactive oxygen species; TUNEL, terminal deoxynucleotidyl transferase-mediated dUTP nick end labeling; z-DEVD-fmk, benzyloxycarbonyl-aspartyl-glutamyl-valyl-aspartyl-fluoromethyl ketone

* Corresponding author. Tel.: +34 957218267; fax: +34 957218229.
E-mail addresses: Giovanni.Appendino@pharm.unipmn.it (G. Appendino), fi1muble@uco.es (E. Muñoz).
[1] Co-corresponding author.

0006-2952/$ – see front matter © 2004 Elsevier Inc. All rights reserved.
doi:10.1016/j.bcp.2004.05.016

Apoptosis is a cell-death machinery characterized in the final phases by chromatin condensation, DNA fragmentation and specific structural changes in cellular structures [8,9]. The selective degradation of cell components in the apoptotic cascade is initiated through the activation of specific cysteine-aspartate proteases called caspases [8], which can be activated either by signaling through cell surface death receptors (such as CD95 or TNFα) or by stimuli that directly target the mitochondria inducing the release to the cytosol of mitochondrial pro-apoptotic components [9]. For instance, it is well known that exposure to calcium ionophores, such as ionomycin or A23187, through the elevation of cytosolic Ca^{2+}, brings to apoptosis in different cell systems [10,11]. Thus, calcium elevation in prelethal concentrations is sufficient to induce mitochondrial Permeability Transition Pore (PTP) opening [12,13], which is closely linked to the induction of apoptosis [14,15]. This PTP is a protein complex formed by the voltage-dependent anion channel (VDAC), the adenine nucleotide translocase (ANT) and cyclophilin-D (CyP-D) at contact sites between the mitochondrial outer and inner membranes [16]. Complete opening of this pore leads to an irreversible dissipation of the mitochondrial transmembrane potential ($\Delta\Psi_m$) that disrupts the mitochondrial structure and leads to the release of proapoptotic factors such as cytochrome-*c* (cyt-*c*), the apoptotic inducing factor (AIF), and the ''inhibitor of apoptosis (IAP)-neutralizing protein'', Diablo [9,14,17]. The immediate consequence of such a release is the formation of the apoptosome, which is formed by cytochrome-*c*, APAF-1, and active caspase-9. Once the apoptosome has assembled, it is able to cleave and activate the effector caspase-3, which is the central caspase responsible for the proteolytic cascade leading to cell death in the majority of cellular systems [9,17]. The open conformation of the PTP seems to be mediated by the switching from a low-conductance to an irreversible high-conductance status that is strictly dependent on the saturation of the internal Ca^{2+}-binding sites of the PTP [18]. Thus, apoptosis induction by PTP-opening is characterized by a loss of the mitochondrial transmembrane potential ($\Delta\Psi_m$) prior to caspase activation.

For decades, plant-derived natural products have been useful for the development of anti-tumoral and anti-inflammatory therapies in modern medicine. In this paper we studied in detail the ionophoretic activity of ferutinin, and we show for the first time the apoptotic mechanisms activated by this daucane sesquiterpene in the Jurkat leukemia cell line.

2. Materials and methods

2.1. Cell lines and reagents

Jurkat cells were maintained in exponential growth in RPMI-1640 medium supplemented with 10% heat inactivated FCS, 2 mM L-glutamine and the antibiotics penicillin and streptomycin (Invitrogen). The cell permeable caspase-3 inhibitor z-DEVD-fmk was from Bachem. Fluorescein isothiocyanate-12-deoxy-2-uridine triphosphate (FITC-dUTP) and terminal deoxynucleotidyltransferase (TdT) were from Roche. The rabbit polyclonal anti-caspase-3 was from Dako Diagnostic. Ferutinin and its derivatives were isolated from giant fennel as previously reported [19]. All other reagents not further specified were from Sigma-Aldrich Química.

2.2. Determination of nuclear DNA loss and cell cycle analysis

The percentage of cells undergoing chromatinolysis (subdiploid cells) was determined after ethanol fixation (70%, for 24 h at 4 °C). The cells were then washed twice with phosphate buffered saline (PBS) solution and subjected to RNA digestion (RNAse-A, 50 U/ml) and PI (20 μg/ml) staining in PBS for 1 h at RT, and analyzed by cytofluorimetry. Under these conditions, low molecular weight DNA leaks from the ethanol-fixed cells and the subsequent staining allows the determination of the percentage of apoptotic cells (sub-G_0/G_1 fraction).

2.3. Detection of DNA strand breaks by the TUNEL method

Cells (1×10^6) were fixed in 4% paraformaldehyde in PBS for 24 h at 4 °C, washed twice in PBS and permeabilized in 0.1% sodium citrate containing 0.1% Triton X-100 for 20 min. Fixed cells were washed three times in PBS and resuspended in a final volume of 50 μl of TUNEL reaction mixture (0.3 nmol FITC-dUTP, 3 nmol dATP, 50 nmol $CoCl_2$, 5 U TdT, 200 mM potassium cacodylate and 250 μg/ml bovine serum albumin in 25 mM Tris–HCl, pH 6.6). The cells were incubated for 1 h at 37 °C and then washed twice in PBS preceding the analysis by flow cytometry. To determine both DNA strand breaks and cell cycle, TUNEL stained cells were counterstained with PI and treated with RNAse as described above prior to cytofluorimetric analysis. In this method, fixation in formaldehyde prevents extraction of low molecular weight DNA from apoptotic cells and thus the cell cycle distribution estimates both apoptotic and non-apoptotic cells.

2.4. Measurement of intracellular free calcium levels ($[Ca^{2+}]_i$)

Cells, at a density of 10^7 cells/ml, were incubated for 1 h at 37 °C in Tyrode's salt solution (composition in mM: 137.0 NaCl, 2.7 KCl, 1.8 $CaCl_2$, 1.0 $MgCl_2$, 0.4 NaH_2PO_4, 12.0 $NaHCO_3$, 5.6 D-glucose) containing 5 μM Indo1-AM (Molecular Probes Europe BV). Cells were then washed three times and resuspended at 2×10^6 cells/ml in

the same buffer. Additional 30 min incubation was made at 37 °C in order to assure the complete intracellular desterification of Indo1-AM, and at the same time, when indicated, in the presence of calcium chelators (BAPTA-AM or EGTA) or calcium-channel inhibitors (nifepidine or verapamil). Immediately after, cells were analyzed in a spectrofluorimeter (Hitachi F-2500 model, Hitachi Ltd.) under continuous stirring and at a constant temperature of 37 °C using a water-jacketed device. After five min accommodation to equilibrate temperatures, samples were excited at 338 nm and emission was collected at 405 and 485 nm, corresponding to the fluorescence emitted by Ca^{2+}-bound and free Indo-1, respectively. $[Ca^{2+}]_i$ was calculated according to Grynkiewicz et al. [20], using the ratio values between bound- and free-Indo-1 fluorescence, and assuming an Indo-1 K_d for Ca^{2+} of 0.23 μM. Maximum and minimum ratio values for calculations were determined by the addition at the end of the measurements of 10 μM ionomycin or 4 mM EGTA, respectively.

2.5. Determination of mitochondrial transmembrane potential and ROS generation

To study the superoxide anion generation (ROS), cells (10^6 ml^{-1}) were incubated in PBS with 2 μM dihydroethidium (HE) (red fluorescent after oxidation) for 20 min at 37 °C, followed by analysis on an Epics XL Analyzer (Coulter). To measure the mitochondrial transmembrane potential ($\Delta\Psi_m$), the cells were incubated in PBS with 20 nM $DiOC_6(3)$ (green fluorescence) (Molecular Probes Europe BV) for 20 min at 37 °C and then analyzed by flow cytometry.

2.6. Determination of caspase-3 activity

Jurkat cells (3×10^6) were washed with PBS and incubated for 30 min on ice with 100 μl of lysis buffer (10 mM Tris–HCl, 10 mM $NaH_2PO_4/NaHPO_4$, pH 7.5, 130 mM NaCl, 1% Triton® X-100, and 10 mM sodium pyrophosphate). Cell lysates were spun, the supernatants collected and the protein concentrations determined by the Bradford method. For each reaction, 30 μg of protein from cell lysates were added to 1 ml of freshly prepared protease assay buffer (20 mM HEPES pH 7.5, 10% glycerol, 2 mM dithiotreitol) containing 20 μM of ac-DEVD-amc (Sigma-Aldrich). Reaction mixtures in the absence of cellular extracts were used as negative controls (fluorescence background). Reaction mixtures were incubated for 1 h at 37 °C and the aminomethyl-coumarin liberated from ac-DEVD-amc was recorded using a spectrofluorimeter (Hitachi F-2500) with an excitation wavelength of 380 nm and an emission wavelength range of 400–550 nm. Data were collected as the integral of relative fluorescence intensity minus the background fluorescence.

2.7. Western blots

Jurkat cells (2×10^6 cells/ml) were washed with PBS and resuspended in 50 μl of lysis buffer (20 mM HEPES pH 8.0, 10 mM KCl, 0.15 mM EGTA, 0.15 mM EDTA, 0.5 mM Na_3VO_4, 5 mM NaFl, 1 mM DTT, leupeptin 1 μg/ml, pepstatin 0.5 μg/ml, apronitin 0.5 μg/ml and 1 mM PMSF) containing 0.5% NP-40. After 15 min on ice, proteins were obtained by centrifugation and the concentration determined by a Bradford assay (Bio-Rad). The proteins (30 μg) were boiled in Laemmli buffer and electrophoresed in 15% SDS–polyacrylamide gels. Separated proteins were transferred to nitrocellulose membranes (0.5 A at 100 V; 4 °C) for 1 h. The blots were further blocked in TBS solution containing 0.1% Tween-20 and 5% nonfat dry milk overnight at 4 °C. Specific proteins were detected with primary rabbit anti-human caspase-3 (Dako Diagnostics), followed with peroxidase linked goat anti-rabbit secondary antibodies (Cell Signalling Technology), and using the luminescent ECL system (Amersham).

3. Results and discussion

3.1. Ferutinin induces Ca^{2+} mobilization in Jurkat cells

We first studied the ionophoretic activity of two compounds isolated from *F. communis* L., ferutinin and ferutidin (Fig. 1), which have previously been shown to act as calcium ionophores [6]. In these experiments we detected that ferutinin induced a rapid $[Ca^{2+}]_i$ increase that was maintained through the time of recording, thereby suggesting that calcium from different sources was mobilized in response to this compound (Fig. 2). On the contrary, a calcium ionophoretic effect was not found with ferutidin, which is in sharp contrast with the results reported by Abramov et al. [6], who showed that ferutidin also promotes dose-dependent increases in conductance for cations

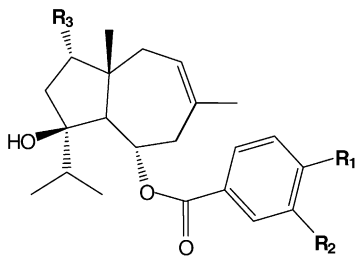

	R_1	R_2	R_3
Ferutinin	OH	H	H
Ferutidin	OMe	H	H
2-α-hydroxyferutidin	OMe	H	OH
Teferin	OH	OMe	H

Fig. 1. Homology in the chemical structures of ferutinin, ferutidin, 2-α-hydroxyferutidin and teferin.

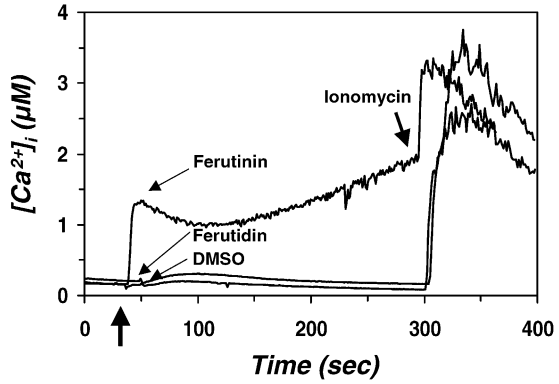

Fig. 2. Effect of ferutinin and ferutidin on intracellular calcium mobilization. Jurkat cells were loaded with Indo1-AM, treated with either ferutinin or ferutidin (50 μM), or solvent alone (DMSO) and the calcium mobilization measured by ratiometric fluorescence as indicated in materials and methods. Vertical arrow indicates the time of compound addition. After 5 min recording, ionomycin (1 μg/ml) was added to standardize results. Data are representative of at least five independent experiments.

in lipid bilayer membranes. However, the differences found in both studies could be due to the use of two different experimental models, isolated lipid bilayer membranes in their study versus intact cells in our experiments. In addition, no competitive or accumulative action was detected when ferutidin was added to the cells prior to ferutinin (data not shown). In order to dissect the biochemical mechanism for this ferutinin-induced calcium mobilization, we examined the effects of EGTA, an extracellular calcium chelator, and BAPTA-AM, which can enter into the cells by mean of the attached acetomethyl group, and when de-esterified by intracellular esterases it is retained inside the cells and becomes a specific calcium chelator. A different pattern of ferutinin-induced calcium mobilization was observed in the presence of either EGTA or BAPTA-AM (Fig. 3A). When cells were treated with BAPTA-AM, the early elevation of intracellular calcium disappeared but a slow calcium accumulation persisted. On the contrary, cells treated with EGTA, which cannot enter the cell, showed the rapid and early phase of calcium mobilization in response to ferutinin, but it disappeared within seconds until it reached the basal levels. These data suggest that ferutinin induces calcium mobilization by at least two different mechanisms, the first one would be mediated by the release of calcium from intracellular stores (inhibited by BAPTA-AM), and the second one mediated by the entry of extracellular calcium, inhibited by EGTA and probably induced by the opening of cell surface calcium channels. The effects of BAPTA as calcium chelator may be sufficient to quench a limited amount of the calcium release to the cytosol (internal stores), but it is not able to quench completely the unusually high $[Ca^{2+}]_i$ induced by ferutinin in Jurkat cells.

The ionophoretic properties of ferutinin have been explained by its incorporation in membranes and by forming a pore selective for calcium and other divalent cations.

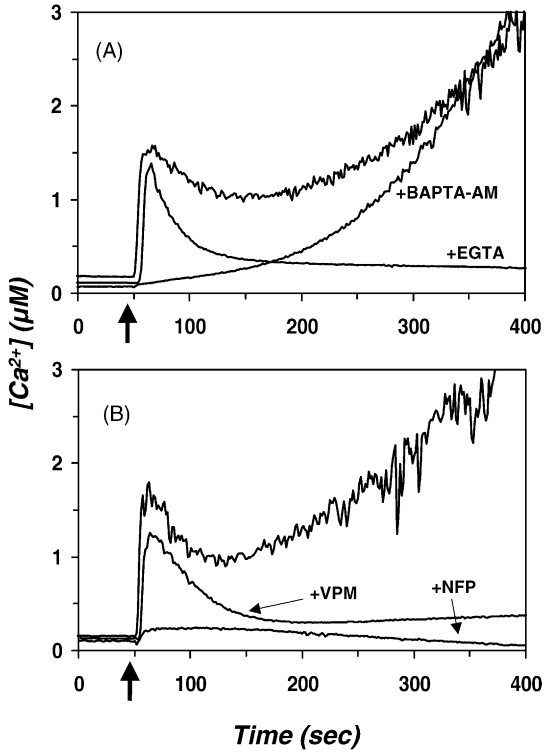

Fig. 3. Effect of calcium chelators and calcium channel blockers on ferutinin-induced calcium mobilization. (A) Jurkat cells were loaded with Indo1-AM as in Fig. 2 and then incubated with either BAPTA-AM (5 μM) or EGTA (2 mM) for 30 min prior to ferutinin treatment (50 μM) (vertical arrow). (B) Indo1-AM loaded cells were pre-incubated with either verapamil (VPM, 20 μM) or nifepidine (NFP, 50 μM), and then treated with ferutinin (50 μM) (vertical arrow). Data are representative of two independent experiments.

This hypothesis assumed an electrogenic transport of calcium following the Nernst's equation [6]. To study the potential role of membrane calcium channels in the ionophoretic activity of ferutinin we performed experiments using the L-type calcium channels blockers verapamil and nifedipine. We showed that both antagonist receptors were able to prevent ferutinin-induced calcium currents, although to a different extent (Fig. 3B), an observation that is not consistent with the reported idea of a direct electrogenic transport of calcium by ferutinin [6]. Therefore, a specific calcium channel seems to be implicated, because a complete inhibition was observed at least with nifedipine. At the moment we cannot explain the different inhibition pattern observed with both L-type channels antagonists. However, some important differences between nifepidine and verapamil in the inhibitory specificity of L-type calcium channels have been reported. For instance, nifedipine is a more potent inhibitor of the α(1-C)b-subunit than of α(1-C)a-subunit of the voltage-dependent L-type Ca^{2+} channel, whereas verapamil is equally potent for both isoforms [21]. Moreover, some authors have questioned the specificity of nifedipine because in several systems, in addition to L-types, it also blocks some intracellular store-operated calcium channels

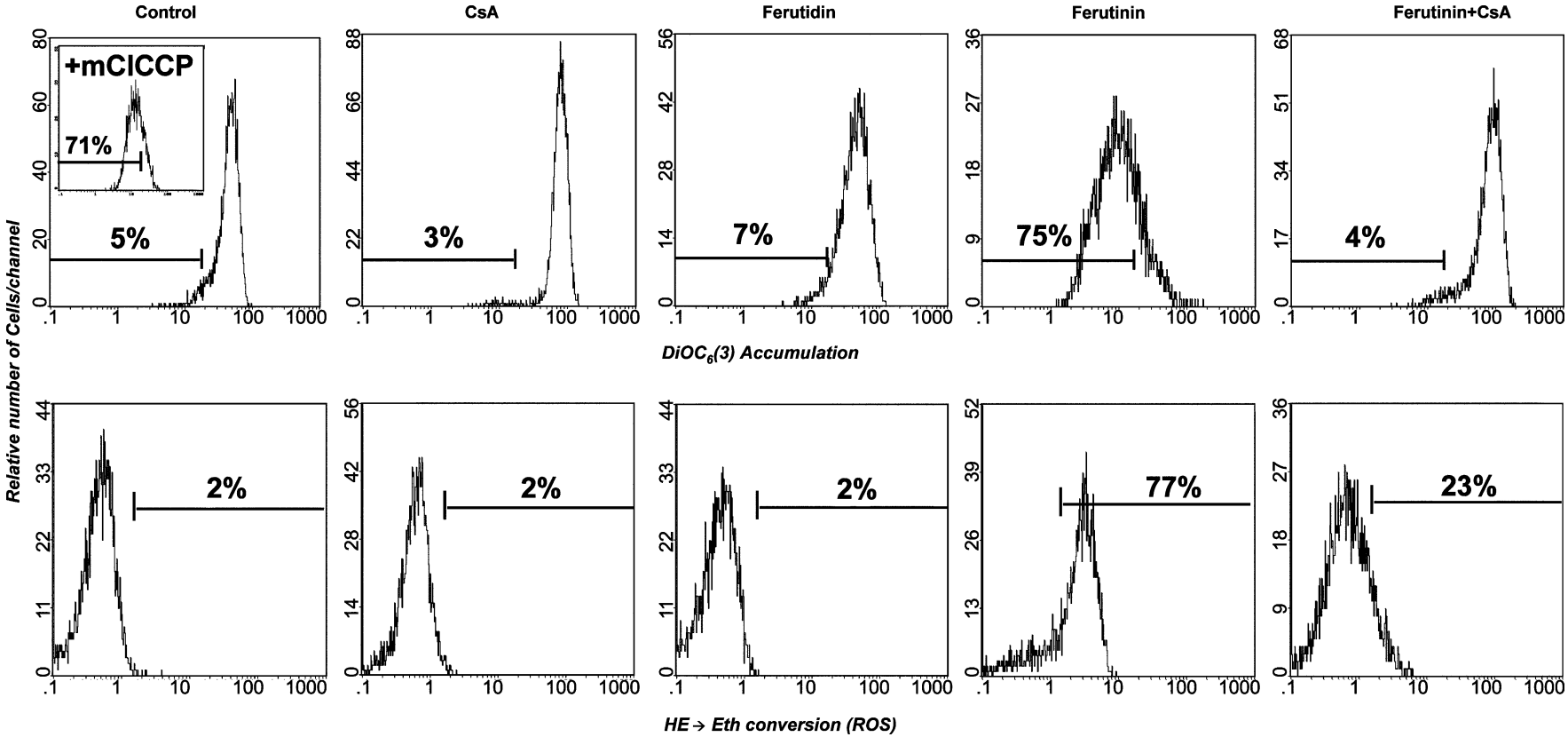

Fig. 4. Effect of ferutinin and ferutidin on the mitochondrial transmembrane potential ($\Delta\Psi_m$) and in ROS generation. $DiOC_6(3)$-loaded Jurkat cells were treated with either CsA (20 μM), ferutidin (50 μM), ferutinin (50 μM) or a combination of ferutinin plus CsA (CsA was added 20 min before ferutinin treatment) for 6 h. In the upper panel the changes in $\Delta\Psi_m$ are measured as the green fluorescence associated to $DiOC_6(3)$ accumulation. The percentage of cells showing decreased $\Delta\Psi_m$ is indicated. The mitochondrial uncoupler cyanide m-chlorophenylhydrazone (mClCCP, 50 μM) is used routinely for validation of measurements (insert in the control histogram). In the lower panel ROS hypergeneration is measured as the increase in red fluorescence following the conversion of dihydroethidium into ethidium by oxygen radicals. Bars represent the percentage of cells showing increased ROS generation. Data are representative of three independent experiments.

[22], and even T-type Ca^{2+}-channels [23]. Thus, further research is warranted to identify the specific ionotropic channels targeted by ferutinin as well as the intracellular binding site for this compound.

3.2. Ferutinin induces $\Delta\Psi_m$ disruption and ROS generation

Numerous data have shown the pro-apoptotic effects of elevated concentrations of intracellular calcium [15,24] and, accordingly, many calcium ionophores are also apoptotic inductors in some cell types [25–27]. Thus, calcium overload has been shown to induce a complete mitochondrial PTP opening [15]. Since ferutinin is a strong calcium ionophore in Jurkat cells, we were interested in studying the mitochondria functionality ($\Delta\Psi_m$ disruption) in ferutinin-treated cells. Thus, for the specific measurement of $\Delta\Psi_m$, Jurkat cells were loaded with the fluorochrome $DiOC_6(3)$, a cationic probe that distributes passively between media, the cytosol and the mitochondria according to the Nernst's equation, where the final distribution of the fluorochrome depends mainly on the transmembrane potential [28]. Compared to control cells, ferutinin-treated cells have a lower $DiOC_6(3)$ fluorescence (a shift to the left in fluorescence intensity), which corresponds with a drop in $\Delta\Psi_m$ (Fig. 4, upper row). As expected, no great changes occurred with ferutidin, in agreement with its lack of ionophoretic and proapoptotic activities, in the Jurkat cell line. Mitochondrial depolarization by itself is not sufficient to demonstrate the PTP opening since uncoupling agents (such as carbonyl cyanide m-chlorophenylhydrazone, mClCCP) do not lead immediately to PTP opening until loss of ATP occurred [29]. Nevertheless, in ferutinin-treated cells the $\Delta\Psi_m$ disruption is related to the PTP opening because a cyclosporin-A (CsA) pretreatment makes the cells resistant to ferutinin-induced mitochondria depolarization. CsA binds to the cyclophilin-D (CyP-D) molecule associated with the matrix side of the PTP, inducing the closure of the pore and preventing $\Delta\Psi_m$ dissipation [30–32]. Thus, it is not surprising that cells treated with CsA showed an increase in $DiOC_6(3)$ fluorescence when compared to untreated control cells, an effect explained by the transient hyperpolarization of the mitochondria caused by the complete PTP closure (Fig. 4) [33–35]. In addition, mitochondrial calcium overload has been linked to an increased generation of reactive oxygen species (ROS) [36]. To study the effects of ferutinin and ferutidin in the generation of ROS in the Jurkat cell line, cells were treated for 6 h as indicated, loaded with the fluorochrome HE, and then the percentage of cells expressing fluorescent Eth was determined by flow cytometry. Ferutinin but not ferutidin induced a high percentage of ROS^+ cells (Fig. 4, lower row). It has been suggested that free $[Ca^{2+}]_i$ is implicated in ROS generation through a Ca^{2+}-dependent protease that converts the xanthine deshydrogenase into xanthine oxydase, which is capable of reducing O_2 to form O_2^-. Thus, it would be possible that a calcium-dependent ROS generation could precede the mitochondrial PTP opening, by oxidizing sulfidryl groups present in the adenine nucleotide translocase (ANT) constituent of PTP [37]. However, it has also been reported that $\Delta\Psi_m$ dissipation, whatever the apoptotic inducing

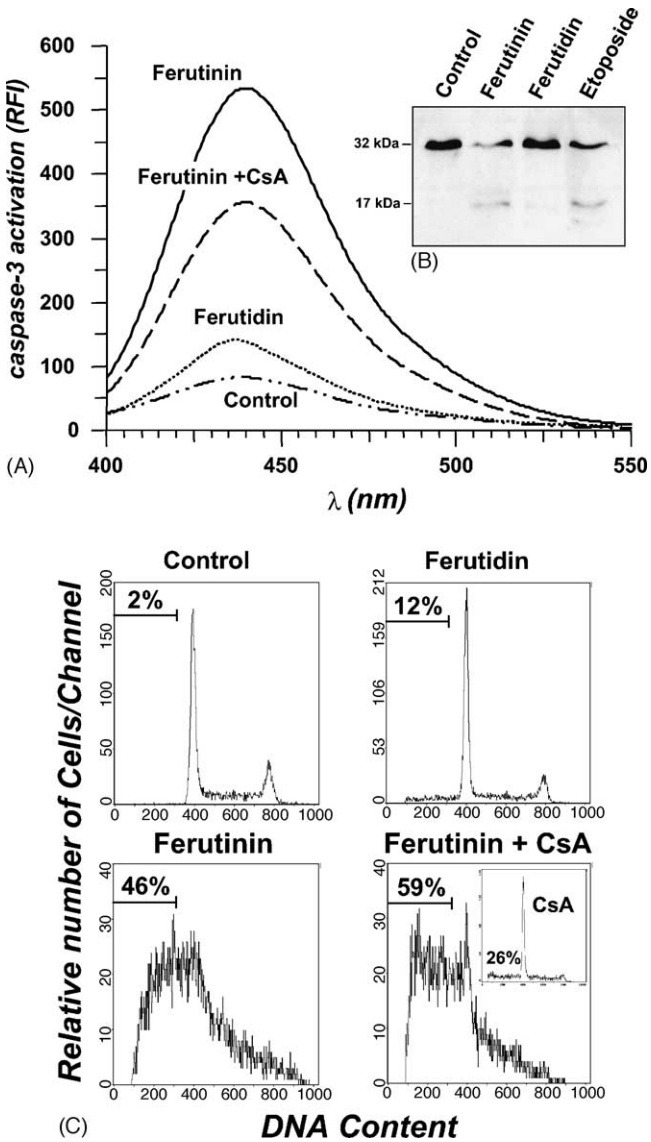

Fig. 5. Effect of ferutinin and ferutidin on the activation of caspase-3 and apoptosis. (A) Caspase-3 activity determination. Jurkat cells were treated for 6 h with either ferutinin (50 μM) in the presence or absence of CsA (20 μM), or with ferutidin (50 μM), and 30 μg protein of each sample were incubated with ac-DEVD-amc. Caspase-3 activation is related to the aminomethyl-coumarin (AMC) liberated and measured by recording the fluorescence emitted after excitation at 380 nm. (B) Studies of caspase-3 cleavage by western blot. Cells were treated with ferutinin (50 μM), ferutidin (50 μM) or Etoposide (20 μM, positive control) for 6h and the steady state protein levels detected by western blot. (C) Determination of the percentage of hypodiploid cells. Jurkat cells were treated as indicated for 18 h and cell cycle analyses studied by flow cytometry. The percentages of hipodyploid cells are indicated. The experiments shown are representative of three (A), one (B) and three (C) independent experiments, respectively.

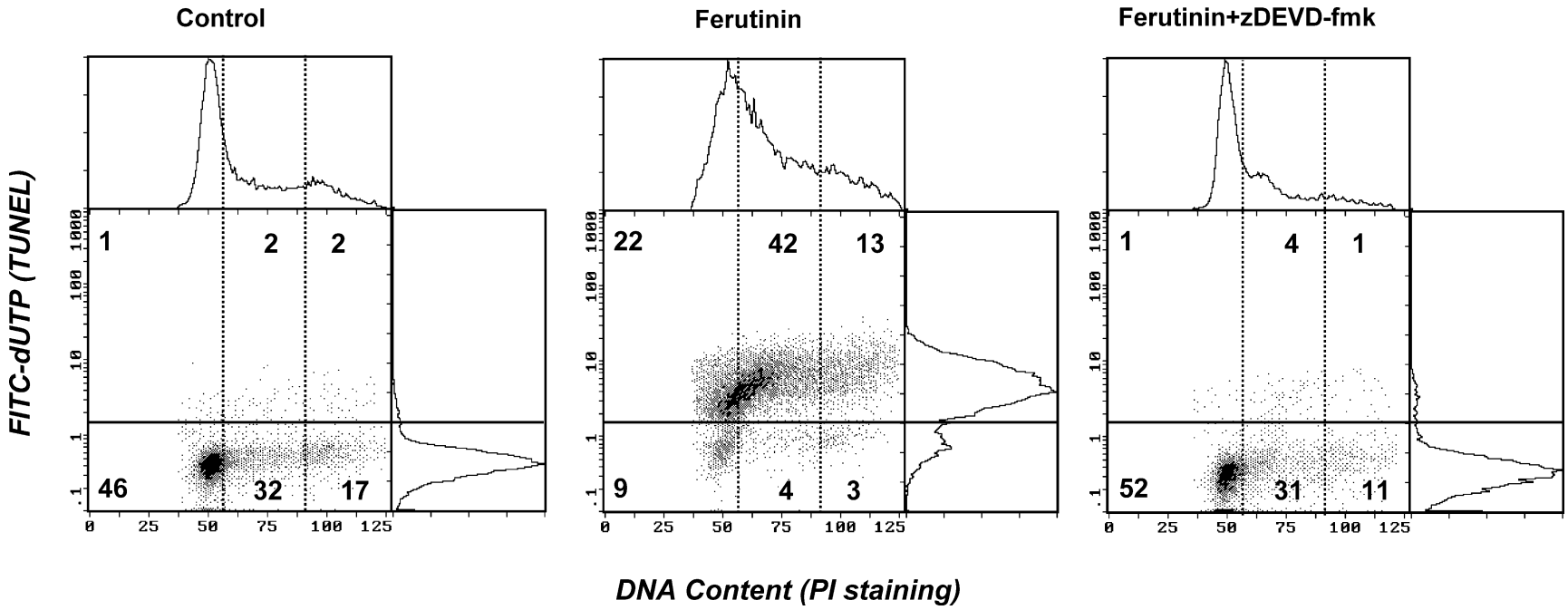

Fig. 6. Ferutinin-induced DNA fragmentation is mediated by caspase-3 and independent of any specific phase of the cell cycle. Jurkat cells were treated with ferutinin (50 μM) in the presence or absence of the caspase-3 inhibitor z-DEVD-fmk (10 μM) for 18 h and the cell cycle (*X*-axis, G_0/G_1, S and G_2/M phases separated by vertical lines) and the DNA strand breaks (TUNEL positive cells, *Y*-axis) were analyzed by flow cytometry. Results are representative of two independent experiments.

agent used, impaired the mitochondrial electron transport chain leading ROS hyperproduction at the level of the complex III of this mitochondrial respiratory chain [38,39]. Our results suggest that ROS are produced after $\Delta\Psi_m$ dissipation in ferutinin-treated cells because CsA not only prevents ferutinin-induced $\Delta\Psi_m$ dissipation but also reduces significantly the percentage of ROS^+ cells (Fig. 4). Nevertheless, the increase of ROS, although secondary to PTP opening, can amplify the apoptotic signal initiated by Ca^{2+}-overload. No inhibition of calcium mobilization was seen with a pretreatment of cells with 20 μM CsA prior to ferutinin exposure (data not shown).

3.3. Ferutinin induces apoptosis through a caspase-3 dependent pathway

A major consequence of the complete PTP opening induced by Ca^{2+} overload is the mitochondrial matrix swelling and the release of pro-apoptogenic factors that in turn activate executor caspases such as the caspase-3 [40]. In order to study whether or not the PTP opening induced by ferutinin was followed by caspase-3 activation, we measured the activity of this cysteinyl-protease by a specific and sensitive spectrofluorometry method. Jurkat cells were treated with either ferutinin or ferutidin for 6 h and the caspase-3 activity was measured in the cell lysates using the fluorogenic tetrapeptide ac-DEVD-amc. As depicted in Fig. 5A, ferutinin clearly activated caspase-3 (over seven-fold more fluorescence than control cells), while the effect of ferutidin on caspase-3 activation was almost negligible (<2-fold increase). In addition, we found by Western blot analyses that etoposide and ferutinin, but not ferutidin, induced the proteolytic cleavage of the 32 kDa procaspase-3 protein (Fig. 5B).

It is remarkable to note that CsA, while capable of inhibiting PTP aperture (Fig. 4), failed to inhibit caspase-3 activation and apoptosis in ferutinin-treated cells. Moreover, CsA alone also induced a significant degree of apoptosis after 18 h in the Jurkat cell line (26% hypodiploidy) (Fig. 5C, insert). It is well known that CsA inhibits PTP opening in short term treatments; however, long term exposure to CsA alone results in the hyperpolarization of the mitochondria and apoptosis in different cell systems [41–43]. This apoptotic effect has been interpreted by some authors as a failure of the mitochondria to maintain ATP/ADP exchange with the cytosol and as a decrease in F_0F_1-ATP synthetase activity due to the complete closure of the voltage-dependent anion channel (VDAC) [33]. Related to this assumption, it is not surprising to find that CsA, despite preventing ferutinin-induced $\Delta\Psi_m$ dissipation (early events), did not protect cells from ferutinin-induced apoptosis (late events).

Taking into account the importance of calcium homeostasis in cell cycle regulation [44,45], we studied whether or not ferutinin-induced apoptosis was associated with any specific phase of the cell cycle. Thus, we performed double staining with PI and FITC-dUTP as described in Section 2. This gives information on the cell cycle phase where DNA fragmentation occurs. In Fig. 6 it is shown that ferutinin-induced DNA fragmentation (77% of the cells) appeared to be proportional to the number of cells in each phase of the cell cycle and was completely prevented with the caspase-3 specific cell-permeable inhibitor, z-DEVD-fmk. Therefore, we cannot ascribe the apoptotic phenomena to any phase of the cell cycle.

Table 1
Apoptosis and calcium mobilization induced by closely related daucane sesquiterpernes

Compound	Apoptosis (%)[a]	Calcium increase (nM)[b]
Ferutinin	40.3	1434 ± 178
Teferin	22.8	1026 ± 103
Ferutidin	7.5	55 ± 2
2-α-Hydroxyferutidin	5.8	94 ± 11

[a] Jurkat cells were treated for 18 h with 50 μM of the indicated compounds. Apoptotic cells were identified as the hypodiploid population detected by flow cytometric cell cycle analyses.

[b] Jurkat cells were loaded with Indo1-AM and incubated with 50 μM of the selected compounds for 30 s at 37 °C. Net increase in $[Ca^{2+}]_i$ was obtained as described in material and methods and by subtracting the basal level of $[Ca^{2+}]_i$ from the peak height after stimulation. Data are the means ± S.D. values of triplicate measurements.

Finally, we compared the ionophoretic and apoptotic activities of ferutinin with the analogues teferin, ferutidin and 2-α-hydroxyferutidin in Jurkat cells. Despite the great similarities between these compounds (Fig. 1), only ferutinin and teferin were able to induce both calcium mobilization and apoptosis (Table 1), thereby indicating that the 4′-hydroxyl group present in these two compounds plays a key role in the biological activities studied in this report. Ferutinin is the major phytoestrogen of plants from the *Ferula* genus, and since severe and unexpected toxicity has been reported for some plants of this genus in animals [1,2], it did not seem unreasonable to assume that ferutinin could also bind to targets different from the estrogen receptors, and we have now discovered that this compound induces calcium mobilization from external and internal stores and eventually triggers apoptosis through a caspase-3 dependent pathway.

Acknowledgments

This work was supported by a contract with the European Commission, grant QLK3-CT-2000-00463 (AINP). A.M. was supported by MCyT grant SAF-2002-01157.

References

[1] Shlosberg A, Egyed MN. Examples of poisonous plants in Israel of importance to animals and man. Arch Toxicol Suppl 1983;6:194–6.
[2] Lamnaouer D. Anticoagulant activity of coumarins from *Ferula communis* L. Therapie 1999;54:747–51.

[3] Ikeda K, Arao Y, Otsuka H, Nomoto S, Horiguchi H, Kato S, et al. Terpenoids found in the *Umbelliferae* family act as agonists/antagonists for ER(alpha) and ER(beta): differential transcription activity between ferutinine-liganded ER(alpha) and ER(beta). Biochem Biophys Res Commun 2002;291:354–60.
[4] Appendino G, Spagliardi P, Cravotto G, Pocock V, Milligan S. Daucane phytoestrogens: a structure–activity study. J Nat Prod 2002;65:1612–5.
[5] Ignatkov V, Akhmedkhodzhaeva Kh S, Babichev VN. The effect of tefestrol on the secretion of luteinizing hormone from the hypophysis. Farmakol Toksikol 1990;53:37–8.
[6] Abramov AY, Zamaraeva MV, Hagelgans AI, Azimov RR, Krasilnikov OV. Influence of plant terpenoids on the permeability of mitochondria and lipid bilayers. Biochim Biophys Acta 2001;1512:98–110.
[7] Abramov AY, Duchen MR. Actions of ionomycin, 4-BrA23187 and a novel electrogenic Ca(2+) ionophore on mitochondria in intact cells. Cell Calcium 2003;33:101–12.
[8] Thornberry NA, Lazebnik Y. Caspases: enemies within. Science 1998;281:1312–6.
[9] Hengartner MO. The biochemistry of apoptosis. Nature 2000; 407:770–6.
[10] Duchen MR. Mitochondria and calcium: from cell signalling to cell death. J Physiol 2000;529(Pt 1):57–68.
[11] McConkey DJ, Orrenius S. The role of calcium in the regulation of apoptosis. Biochem Biophys Res Commun 1997;239:357–66.
[12] Azzi A, Azzone GF. Swelling and shrinkage phenomena in liver mitochondria. 3. Irreversible swelling induced by inorganic phosphate and Ca^{2+}. Biochim Biophys Acta 1966;113:438–44.
[13] Hoek JB, Farber JL, Thomas AP, Wang X. Calcium ion-dependent signalling and mitochondrial dysfunction: mitochondrial calcium uptake during hormonal stimulation in intact liver cells and its implication for the mitochondrial permeability transition. Biochim Biophys Acta 1995;1271:93–102.
[14] Kroemer G, Dallaporta B, Rescherigon M. The mitochondrial death/life regulator in apoptosis and necrosis. Annu Rev Physiol 1998;60:619–42.
[15] Crompton M. The mitochondrial permeability transition pore and its role in cell death. Biochem J 1999;341:233–49.
[16] Halestrap AP, Brennerb C. The adenine nucleotide translocase: a central component of the mitochondrial permeability transition pore and key player in cell death. Curr Med Chem 2003;10:1507–25.
[17] Green DR, Reed JC. Mitochondria and apoptosis. Science 1998;281:1309–16.
[18] Ichas F, Mazat JP. From calcium signaling to cell death: two conformations for the mitochondrial permeability transition pore. Switching from low- to high-conductance state. Biochim Biophys Acta 1998;1366:33–50.
[19] Appendino G, Cravotto G, Sterner O, Ballero M. Oxygenated sesquiterpenoids from a nonpoisonous sardinian chemotype of giant fennel (*Ferula communis*). J Nat Prod 2001;64:393–5.
[20] Grynkiewicz G, Poenie M, Tsien RY. A new generation of Ca^{2+} indicators with greatly improved fluorescence properties. J Biol Chem 1985;260:3440–50.
[21] Morel N, Buryi V, Feron O, Gomez JP, Christen MO, Godfraind T. The action of calcium channel blockers on recombinant L-type calcium channel alpha1-subunits. Br J Pharmacol 1998;125:1005–12.
[22] Curtis TM, Scholfield CN. Nifedipine blocks Ca^{2+} store refilling through a pathway not involving L-type Ca^{2+} channels in rabbit arteriolar smooth muscle. J Physiol 2001;532:609–23.
[23] McDonald TF, Pelzer S, Trautwein W, Pelzer DJ. Regulation and modulation of calcium channels in cardiac, skeletal, and smooth muscle cells. Physiol Rev 1994;74:365–507.
[24] Nicotera P, Orrenius S. The role of calcium in apoptosis. Cell Calcium 1998;23:173–80.
[25] Wyllie AH, Morris RG, Smith AL, Dunlop D. Chromatin cleavage in apoptosis: association with condensed chromatin morphology and dependence on macromolecular synthesis. J Pathol 1984;142:67–77.
[26] Martikainen P, Isaacs J. Role of calcium in the programmed death of rat prostatic glandular cells. Prostate 1990;17:175–87.
[27] Takadera T, Ohyashiki T. Apoptotic cell death and caspase 3 (CPP32) activation induced by calcium ionophore at low concentrations and their prevention by nerve growth factor in PC12 cells. Eur J Biochem 1997;249:8–12.
[28] Petit PX, O'Connor JE, Grunwald D, Brown SC. Analysis of the membrane potential of rat- and mouse-liver mitochondria by flow cytometry and possible applications. Eur J Biochem 1990;194: 389–97.
[29] Nieminen AL, Saylor AK, Tesfai SA, Herman B, Lemasters JJ. Contribution of the mitochondrial permeability transition to lethal injury after exposure of hepatocytes to *t*-butylhydroperoxide. Biochem J 1995;307(Pt 1):99–106.
[30] Halestrap AP, Davidson AM. Inhibition of Ca^{2+}-induced large-amplitute swelling of liver and heart mitochondria by cyclosporin is probably caused by the inhibitor binding to mitochondrial-matrix peptidyl-prolyl *cis-trans* isomerase and preventing it interacting with the adenine nucleotide translocase. Biochem J 1990;268:153–60.
[31] Crompton M, McGuinness O, Nazareth W. The involvement of cyclosporin A binding proteins in regulating and uncoupling mitochondrial energy transduction. Biochim Biophys Acta 1992;1101:214–7.
[32] Woodfield K, Ruck A, Brdiczka D, Halestrap AP. Direct demonstration of a specific interaction between cyclophilin-D and the adenine nucleotide translocase confirms their role in the mitochondrial permeability transition. Biochem J 1998;336:287–90.
[33] Ly JD, Grubb DR, Lawen A. The mitochondrial membrane potential (Deltapsi(m)) in apoptosis an update. Apoptosis 2003;8:115–28.
[34] Vander Heiden MG, Chandel NS, Schumacker PT, Thompson CB. Bcl-XL prevents cell death following growth factor withdrawal by facilitating mitochondrial ATP/ADP exchange. Mol Cell 1999;3:159–67.
[35] Scarlett JL, Sheard PW, Hughes G, Ledgerwood EC, Ku HH, Murphy MP. Changes in mitochondrial membrane potential during staurosporine-induced apoptosis in Jurkat cells. FEBS Lett 2000;475:267–72.
[36] Lemasters JJ, Nieminen AL. Mitochondrial oxygen radical formation during reductive and oxidative stress to intact hepatocytes. Biosci Rep 1997;17:281–91.
[37] Halestrap AP, Kerr PM, Javadov S, Woodfield KY. Elucidating the molecular mechanism of the permeability transition pore and its role in reperfusion injury of the heart. Biochim Biophys Acta 1998;1366:79–94.
[38] Castedo M, Macho A, Zamzami N, Hirsch T, Marchetti P, Uriel J, et al. Mitochondrial perturbations define lymphocytes undergoing apoptotic depletion in vivo. Eur J Immunol 1996;25:3277–84.
[39] Zamzami N, Marchetti P, Castedo M, Decaudin D, Macho A, Hirsch T, et al. Sequential reduction of mitochondrial transmembrane potential and generation of reactive oxygen species in early programmed cell death. J Exp Med 1995;182:367–77.
[40] Gogvadze V, Robertson JD, Zhivotovsky B, Orrenius S. Cytochrome *c* release occurs via Ca^{2+}-dependent and Ca^{2+}-independent mechanisms that are regulated by Bax. J Biol Chem 2001;276:19066–71.
[41] Naujokat C, Daniel V, Bauer TM, Sadeghi M, Opelz G. Cell cycle- and activation-dependent regulation of cyclosporin A-induced T cell apoptosis. Biochem Biophys Res Commun 2003;310:347–54.
[42] Fornoni A, Li H, Foschi A, Striker GE, Striker LJ. Hepatocyte growth factor, but not insulin-like growth factor I, protects podocytes against cyclosporin A-induced apoptosis. Am J Pathol 2001;158:275–80.
[43] Ortiz A, Lorz C, Catalan M, Coca S, Egido J. Cyclosporine A induces apoptosis in murine tubular epithelial cells: role of caspases. Kidney Int Suppl 1998;68:S25–9.
[44] Norris V, Ayala JA, Begg K, Bouche JP, Bouloc P, Boye E, et al. Cell cycle control: prokaryotic solutions to eukaryotic problems? J Theor Biol 1994;168:227–30.
[45] Silver RB. Calcium and cellular clocks orchestrate cell division. Ann NY Acad Sci 1990;582:207–21.